

*Journal of*  
***Mechanics of***  
***Materials and Structures***

**DETERMINATION OF STRAIN GAGE LOCATIONS FOR THE  
ACCURATE MEASUREMENT OF OPENING MODE STRESS  
INTENSITY FACTORS**

B. Kaushik, K. S. R. K. Murthy and P. S. Robi

***Volume 3, N<sup>o</sup> 9***

***November 2008***



mathematical sciences publishers

## DETERMINATION OF STRAIN GAGE LOCATIONS FOR THE ACCURATE MEASUREMENT OF OPENING MODE STRESS INTENSITY FACTORS

B. KAUSHIK, K. S. R. K. MURTHY AND P. S. ROBI

The accuracy of measurement of opening mode stress intensity factors using the strain gage techniques largely depends on location of the gages. The radial position of the strain gages is a major issue in measurement of the stress intensity factors. This paper describes an approach to resolve this problem. The present work proposes a method for practically accurate determination of a vital parameter designated as ( $r_{\max}$ ) which in turn is extremely useful in judging the valid positions of the strain gages. The results of the present investigation clearly show that the proposed method is simple and accurate values of  $r_{\max}$  can be determined.

### 1. Introduction

The stress intensity factor (SIF) is extensively employed when applying the principles of linear elastic fracture mechanics (LEFM) to the analysis of the safety of engineering components containing cracks. It is used to understand the severity of the cracks while calculating the static strength, fatigue crack growth and life predictions. The SIF is of considerable importance in many engineering situations, since the critical value of this parameter determines whether or not the existing crack will propagate.

The use of LEFM principles in preventing the fracture of engineering components depends largely on the availability of accurate SIFs. As a result, analytical, numerical and experimental methods for SIF determination in cracked bodies have been developed over the years.

Experimental methods, in particular, play an important role in complex situations [Sanford 2003] and are essential to the validation and correct application of theoretical and numerical results. They include the compliance method [Bonesteel et al. 1978; Newman 1981], photoelasticity [Gdoutos and Theocaris 1978; Hyde and Warrior 1990], caustics [Theocaris 1970; Konsta-Gdoutos 1996] and strain gage methods [Dally and Berger 1993; Swamy et al. 2008]. Among these, the strain gage technique is relatively simple and straightforward [Sanford 2003].

Four strain gage techniques [Dally and Sanford 1987; Wei and Zhao 1997; Kuang and Chen 1995; Berger and Dally 1988] are currently available for experimental determination of mode I stress intensity factors under static loading. Factors such as the local yielding effect at the crack tip, high strain gradients, the three-dimensional state of stress at the crack tips and the finite size of the strain gages strongly affect the performance of strain gage techniques.

Dally and Sanford [1987] were the first to develop a strain gage technique for measuring the static opening mode stress intensity factor ( $K_I$ ) in two dimensional isotropic bodies which overcomes these difficulties. This was achieved by identifying the valid region around the crack tip for accurate measurement of the strains. These authors proposed to determine the mode I SIF using a truncated strain

*Keywords:* stress intensity factors, cracks, fracture, strain gage, finite element analysis.

series containing only three parameters. The chief advantage of their approach is that only one strain gage is sufficient to determine the mode I SIF, by locating it at distances far away from the crack tip. However, the radial location of the strain gage should be within the realm of applicability of the three-parameter representation. Thus this technique requires knowing beforehand the extent of validity of the three-parameter representation. In general, this extent depends on configuration and boundary conditions; no suggestions were made in [Dally and Sanford 1987] toward this end.

[Wei and Zhao 1997] and [Kuang and Chen 1995] devised different strain gage methods for measuring the static mode I SIF. Two strain gages are needed for measuring the opening mode SIF in the approach in the first of these papers. However, locations (radial distances) of the strain gages are suggested empirically and necessitate a priori knowledge about the plastic zone size, which depends on the unknown stress intensity factor of the configuration.

In contrast, [Kuang and Chen 1995] used asymptotic strain expressions for the measurement of the mode I SIF. They suggested that strain gages can be placed at distances greater than half the thickness of the specimen from the crack tip despite the fact that at large distances from the crack tip the measured strains cannot be accurately represented by asymptotic terms alone. Their results show that the measured normalized SIF is a function of the applied loads, the thickness of the specimen and the angular position  $\theta$  from the crack axis.

A very large number of strain gages is needed to measure the opening mode SIFs in an overdeterministic method proposed in [Berger and Dally 1988]. Among these techniques, the single strain gage method [Dally and Sanford 1987] is most popular.

Apart from development of various techniques, another important direction in experimental determination of static stress intensity factors is the application of the existing techniques to corroborate the analytical/numerical solutions of the SIFs. For example, application of photoelastic methods is dealt in [Marloff et al. 1971; Chan and Chow 1979; Kazemi et al. 1989; Nurse et al. 1994] and caustics techniques in [Baik et al. 1995; Lee and Hong 1993]. Such investigations establish the existing techniques as useful tools in real design situations of great complexity. In spite of these potential applications of the strain gage methods, very limited work has been reported to date [Swamy et al. 2008], particularly on applications of Dally and Sanford's single strain gage procedure in order to validate/suggest accurate mode I, static SIFs of the complex configurations. This is true even in case of the other strain gage methods.

One important reason which hampered the potential application of Dally and Sanford's method is the uncertainty over the radial location ( $r$ ) of the strain gage, where ( $r$ ) is the radial distance from the crack tip. Improper locations may lead to highly erroneous measurement of the surface strains. Theoretically, the three-parameter strain series of Dally and Sanford accurately estimates the strain field up to a certain radial distance, say  $r_{\max}$  (depending on the angular position  $\theta$ ) from the crack tip. This distance depends on the given configuration and boundary conditions. As a result this quantity is not known a priori. From the strain gradient analysis in [Dally and Sanford 1987] and the behavior of a crack with a plastic zone ahead of it [Sanford 2003], it is preferable to paste the gages far way from the crack tip but not beyond  $r_{\max}$ . Therefore, it is evident that the knowledge of  $r_{\max}$  is essential before conducting the experiments so as to access whether the selected radial distance of the strain gage is meeting the above requirement or not. If the chosen or guessed value of  $r$  is small then the measured strains may be severely affected due to plasticity and strain gradient effects. On the other hand if it is greater than the unknown  $r_{\max}$ , though the above errors decrease rapidly but the measured strains may not be as per the theoretical predictions.

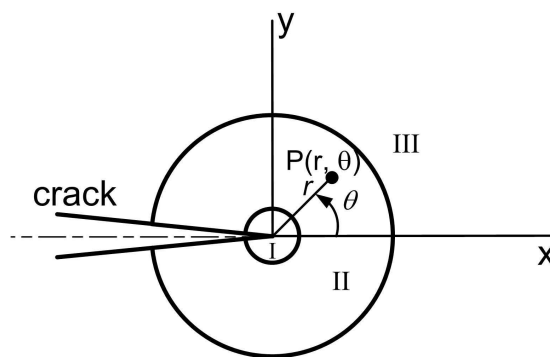


**Figure 1.** Various regions at the crack tip [Dally and Sanford 1987].

It is worth noting that, at least a reasonably approximate value of the extent of validity of three-parameter strain series or  $r_{\max}$  is therefore needed for properly locating the gages. To the best of authors' knowledge no means are currently available to estimate the value of  $r_{\max}$  in order to measure accurate opening mode SIFs using the approach of [Dally and Sanford 1987].

The present work attempts to suggest a computational approach to determine reasonably accurate values of  $r_{\max}$  of a given configuration in line with the method of Dally and Sanford. The solution is presented using the finite element analysis of cracked specimens. Single edge cracked plate problems are considered with finite width and height to demonstrate the present approach. The outline of the paper is as follows. First, theoretical background for numerical determination of  $r_{\max}$  is presented in Section 2. Section 3 presents numerical examples to demonstrate the proposed approach for determination of  $r_{\max}$ . Finally some concluding remarks are summarized in Section 3.

## 2. Theoretical background

The main underlying idea behind single strain gage technique of [Dally and Sanford 1987] is identification of a suitable region around the crack tip within which accurate measurement of surface strains can be made. Therefore, the region around a crack tip (traction free crack faces) is divided into three zones viz. very near field, near field and far field zones as shown in Figure 1.

The very near field zone is close to the crack tip and first term of the strain series (singular strain term) is sufficient to represent the strains. However, it is not a valid zone for accurate strain measurements as the stress state in this region is three-dimensional (neither plane stress nor plane strain) [Rosakis and Ravi-Chandar 1986] and the measured strains will be severely affected by plasticity effects. Also errors in measuring the position of the strain gage are excessive if they are located very close to the crack tip.

The far field zone is again not suitable for collection of strain data because very large number of terms in the strain series is required to yield accurate results. Therefore, Dally and Sanford identified that the intermediate or near field zone is favorable and optimum zone for accurate measurement of the surface strains. In this zone, a singular term and a small number of higher order terms accurately describe the strain field.

The near field strain equations are obtained using the generalized Westergaard approach proposed by [Sanford 1979]. The modified Airy stress function in this approach is given by

$$\phi = \operatorname{Re} \bar{\bar{Z}}(z) + y \operatorname{Im} \bar{Z}(z) + \operatorname{Im} \bar{Y}(z), \quad (1)$$

where

$$\frac{d\bar{\bar{Z}}}{dz} = \bar{Z}, \quad \frac{d\bar{Z}}{dz} = Z, \quad \frac{d\bar{Y}}{dz} = Y \quad (2)$$

and the complex analytic functions  $Z(z)$  and  $Y(z)$  are defined as

$$Z(z) = \sum_{n=0}^{\infty} A_n z^{(n-1)/2} = \frac{K}{\sqrt{2\pi z}} + \sum_{n=1}^{\infty} A_n z^{(n-1)/2}, \quad Y(z) = \sum_{m=0}^{\infty} B_m z^m = \frac{\sigma_{0x}}{2} + \sum_{m=1}^{\infty} B_m z^m, \quad (3)$$

which are series type functions (in terms of the complex variable  $z = x + iy$ ) containing an infinite number of coefficients  $A_1, A_2, \dots, B_1, B_2, \dots$  that can be determined using the boundary conditions of a given problem. The stress components for the entire domain are represented by Dally and Sanford as

$$\begin{aligned} \sigma_{xx} &= \operatorname{Re} Z - y \operatorname{Im} Z' - y \operatorname{Im} Y' + 2 \operatorname{Re} Y, \\ \sigma_{yy} &= \operatorname{Re} Z + y \operatorname{Im} Z' + y \operatorname{Im} Y', \\ \tau_{xy} &= -y \operatorname{Re} Z' - y \operatorname{Re} Y' - \operatorname{Im} Y. \end{aligned} \quad (4)$$

Assuming plane stress conditions, the stress-strain relations are given by

$$\varepsilon_{xx} = \frac{1}{E}(\sigma_{xx} - \nu\sigma_{yy}), \quad \varepsilon_{yy} = \frac{1}{E}(\sigma_{yy} - \nu\sigma_{xx}), \quad \gamma_{xy} = \frac{\tau_{xy}}{G}. \quad (5)$$

Equations for the strain field can be obtained upon substituting (4) in (5)

$$E\varepsilon_{xx} = (1 - \nu) \operatorname{Re} Z - (1 + \nu)y \operatorname{Im} Z' - (1 + \nu)y \operatorname{Im} Y' + 2 \operatorname{Re} Y \quad (6a)$$

$$E\varepsilon_{yy} = (1 - \nu) \operatorname{Re} Z + (1 + \nu)y \operatorname{Im} Z' + (1 + \nu)y \operatorname{Im} Y' - 2\nu \operatorname{Re} Y \quad (6b)$$

$$G\gamma_{xy} = -y \operatorname{Re} Y' - \operatorname{Im} Y - y \operatorname{Re} Z' \quad (6c)$$

Substitution of series form of complex functions  $Z(z)$  and  $Y(z)$  from (3) gives exact representation of strain field in the domain with infinite number of unknown coefficients  $A_n$  and  $B_m$ . It is assumed that the strain field in the near field zone can be sufficiently represented by the three-parameter series with unknown coefficients  $A_0, A_1$  and  $B_0$ . The three-term representation of strain field in this region is therefore

$$E\varepsilon_{xx} = A_0 r^{-1/2} \cos \frac{\theta}{2} \left( (1 - \nu) - (1 + \nu) \sin \frac{\theta}{2} \sin \frac{3\theta}{2} \right) + 2B_0 + A_1 r^{1/2} \cos \frac{\theta}{2} \left( (1 - \nu) + (1 + \nu) \sin^2 \frac{\theta}{2} \right),$$

$$E\varepsilon_{yy} = A_0 r^{-1/2} \cos \frac{\theta}{2} \left( (1 - \nu) + (1 + \nu) \sin \frac{\theta}{2} \sin \frac{3\theta}{2} \right) - 2\nu B_0 + A_1 r^{1/2} \cos \frac{\theta}{2} \left( (1 - \nu) - (1 + \nu) \sin^2 \frac{\theta}{2} \right),$$

$$2G\gamma_{xy} = A_0 r^{-1/2} \left( \sin \theta \cos \frac{3\theta}{2} \right) - A_1 r^{1/2} \left( \sin \theta \cos \frac{\theta}{2} \right),$$

where  $A_0, A_1$  and  $B_0$  are unknown coefficients that can be determined using the geometry of the specimen and the boundary conditions. Using the definition of  $K_I$  one can easily show that it is related to  $A_0$  by

$$K_I = \sqrt{2\pi} A_0. \quad (7)$$

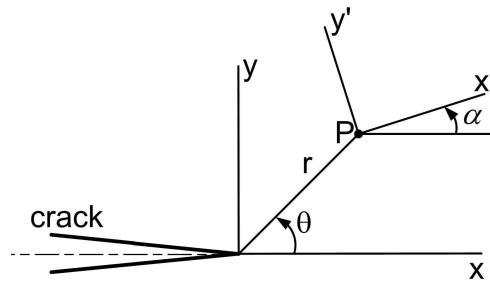


**Figure 2.** Strain gage location and orientation [Dally and Sanford 1987].

A single strain gage is sufficient to measure the constant  $A_0$  (hence  $K_I$ ) by placing and orienting the strain gage as given below.

Using the strain transformation equations, the strain component  $\varepsilon_{x'x'}$  at the point  $P$  located by  $r$  and  $\theta$  (Figure 2) is given by

$$2G\varepsilon_{x'x'} = A_0r^{-1/2} \left( \kappa \cos \frac{\theta}{2} - \frac{1}{2} \sin \theta \sin \frac{3\theta}{2} \cos 2\alpha + \frac{1}{2} \sin \theta \cos \frac{3\theta}{2} \sin 2\alpha \right) + B_0(\kappa + \cos 2\alpha) + A_1r^{1/2} \cos \frac{\theta}{2} \left( \kappa + \sin^2 \frac{\theta}{2} \cos 2\alpha - \frac{1}{2} \sin \theta \sin 2\alpha \right), \quad (8)$$

where  $\kappa = \frac{1-\nu}{1+\nu}$ . The  $B_0$  term in this equation can be eliminated by selecting the angle  $\alpha$  so that

$$\cos 2\alpha = -\kappa = -\frac{1-\nu}{1+\nu}. \quad (9)$$

Similarly the coefficient  $A_1$  vanishes if the angle  $\theta$  is chosen so that

$$\tan \frac{\theta}{2} = -\cot 2\alpha. \quad (10)$$

Thus by placing a single strain gage (Figure 2) with  $\alpha$  and  $\theta$  as defined by (9) and (10) one can measure the strain  $\varepsilon_{x'x'}$ , which in turn is related to  $K_I$  by

$$\varepsilon_{x'x'} = \frac{1}{\sqrt{r}} \left[ \frac{K_I}{G\sqrt{8\pi}} \left( \kappa \cos \frac{\theta}{2} - \frac{1}{2} \sin \theta \sin \frac{3\theta}{2} \cos 2\alpha + \frac{1}{2} \sin \theta \cos \frac{3\theta}{2} \sin 2\alpha \right) \right]. \quad (11)$$

This equation accurately determines  $\varepsilon_{x'x'}$  up to a radial distance of  $r_{\max}$ . For a given configuration, applied load, Young’s modulus  $E$  and Poisson’s ratio  $\nu$ , the bracketed part on right-hand side of (11) is a constant. Therefore

$$\varepsilon_{x'x'} = \frac{C}{\sqrt{r}}, \quad (12)$$

where  $C$  is a constant. Taking the logarithm on both sides of (12) we get

$$\ln \varepsilon_{x'x'} = -\frac{1}{2} \ln r + \ln C. \quad (13)$$

Equations (12) and (13) are valid along the line given by (10) until a radial distance of  $r_{\max}$ . Thus a log-log plot of (12) is a straight line of slope  $-0.5$ , with an intercept of  $\ln C$ . The straight line property generally breaks for  $r > r_{\max}$ , because then more than three parameters are needed in (8) to estimate  $\varepsilon_{x'x'}$ . Using (13), the value of  $r_{\max}$  can be accurately estimated.

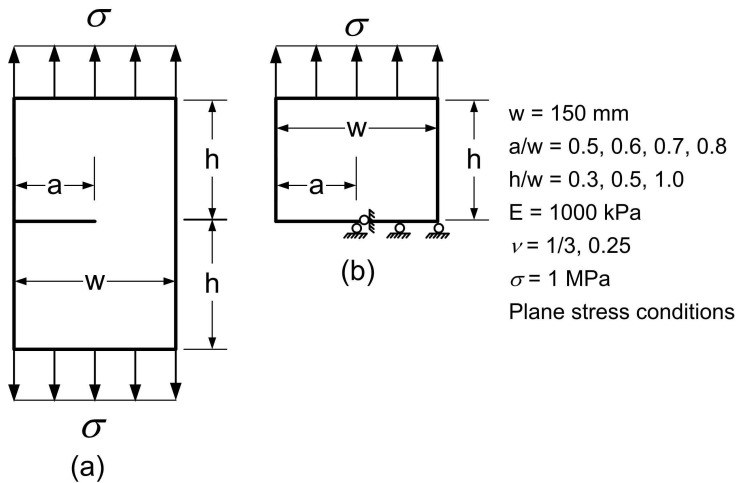


**Figure 3.** (a) Problem domain: Finite edge cracked plate subjected to uniform tension; (b) half-model along with the symmetry boundary conditions used for the finite element analysis.

### 3. Numerical examples

This section describes the proposed approach based on the finite element analysis of a given cracked configuration for reasonably accurate estimation of the corresponding  $r_{\max}$ . The method is presented with the aid of numerical examples. For this purpose finite width and finite height edge cracked plates subjected to uniform tensile stress are considered; see Figure 3(a). Due to symmetry only half the plate is modeled, as shown in Figure 3(b). We generate different configurations, with  $a/w = 0.5, 0.6, 0.7, 0.8$  and  $h/w = 0.3, 0.5, 1.0$ . The width  $w = 150 \text{ mm}$  of the plate is fixed in all cases, as is the value of  $1000 \text{ kPa}$  for Young's modulus. Plane stress conditions are assumed. ANSYS 9 and 11 was used for the finite element analysis, with eight noded isoparametric quadrilateral elements (Q8). The crack tip is modelled by collapsed Q8 quarter-point elements [Barsoum 1976].

**Example 1: Determination of  $r_{\max}$  using finite element analysis.** The primary purpose of this example is to demonstrate the basic procedure for determination reasonably accurate values of  $r_{\max}$  of a configuration. The procedure is described using the edge cracked plates subjected to uniform tensile stress as shown in Figure 3(a) with  $a/w = 0.5$  and  $h/w = 0.3, 0.5, 1.0$ . A Poisson's ratio of  $\nu = 1/3$  and an applied stress value of  $1.0 \text{ MPa}$  are assumed for all three configurations. For  $\nu = 1/3$ , the values of  $\theta$  and  $\alpha$  both equal  $60^\circ$ ; see (9) and (10). To study the effect of mesh refinement on the convergence of  $r_{\max}$ , three meshes of increasing density are considered for each configuration; see Figures 4–6.

The meshes are designed so that nodes of several elements are made to lie along the radial line which makes an angle of  $\theta$  with the horizontal ( $60^\circ$  for  $\nu = 1/3$ ). This line begins at the crack-tip and terminates at the outer boundaries of the cracked plate. It should be noted that according to [Dally and Sanford 1987], a single strain gage is required to be placed at an appropriate location on this line in the direction of  $\alpha$  in order to measure the linear strain  $\varepsilon_{x'x'}$  (Figure 2). We call this the *gage-line*. The computed strains in the global coordinates (using the finite element analysis) along the gage line are then transformed to

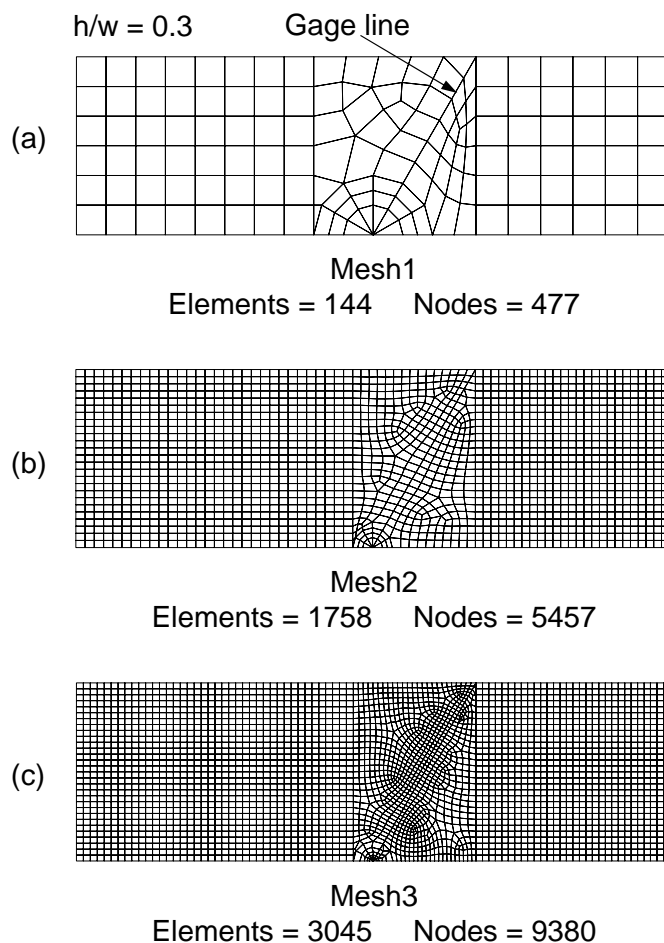


**Figure 4.** Different finite element meshes used for convergence study of  $r_{\max}$  of  $a/w = 0.5$  and  $h/w = 0.3$  edge cracked configuration.

the linear strain  $\varepsilon_{x'x'}$  in the direction defined by  $\alpha = 60^\circ$ ; see (8). The radial distances ( $r$ ) of each of the nodes on the gage line from the crack tip are then computed.

Figures 7 and 8 show plots of  $\log \varepsilon_{x'x'}$  as a function of  $\log r$ , computed from each of the three meshes of  $h/w = 0.3, 0.5, 1.0$ . The crack tip point is not plotted, as the radius of this point is zero. It is interesting to notice from all the plots of Figures 7 and 8 that the linear trend in logarithmic axes distinctly exists until a radial distance. This trend can be clearly observed in all the three meshes of each of the  $h/w$  value. The results presented in Figures 7 and 8 also strongly confirm that the selection of coefficients ( $A_0, B_0, A_1$ ) that are retained in the three-parameter strain series (8) appears to be valid. The end point of the linear portion of the plots (Figures 7 and 8) clearly indicates the terminal point of validity of the three-parameter strain series (8) or  $r_{\max}$  in accordance with the single gage approach of [Dally and Sanford 1987]—see (13).

Since the  $\varepsilon_{x'x'}$  values are obtained numerically, we see that the slope of a line segment between any two data points (Figures 7 and 8) belonging to the fine meshes is close to the theoretical value of  $-0.5$  (13)—

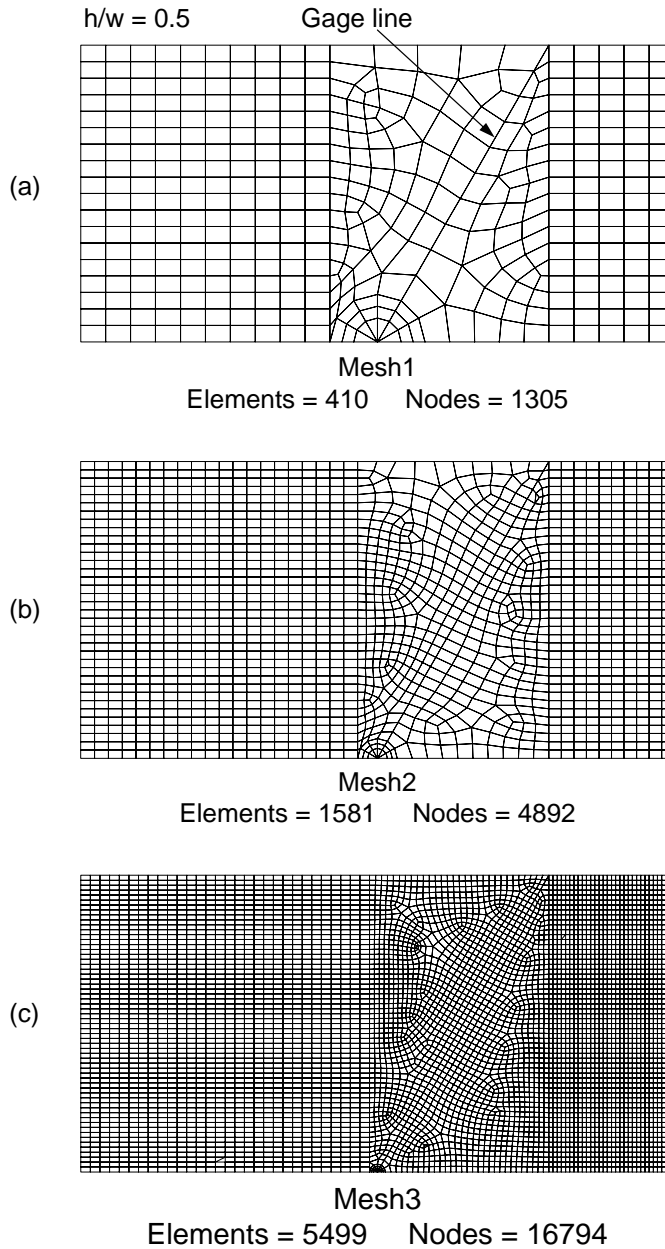


**Figure 5.** Different finite element meshes used for convergence study of  $r_{\max}$  of  $a/w = 0.5$  and  $h/w = 0.5$  edge cracked configuration.

more so than for coarse meshes. A line of slope  $-0.5$  is included in Figures 7 and 8 for comparison. Thus a reasonably accurate value of  $r_{\max}$  can be estimated as the terminal point of the straight line portion on logarithmic axes. These terminal points are also indicated in Figures 7 and 8. The precise value of  $r_{\max}$  is not essential for locating the strain gages, because they do not have to be placed precisely at  $r_{\max}$ .

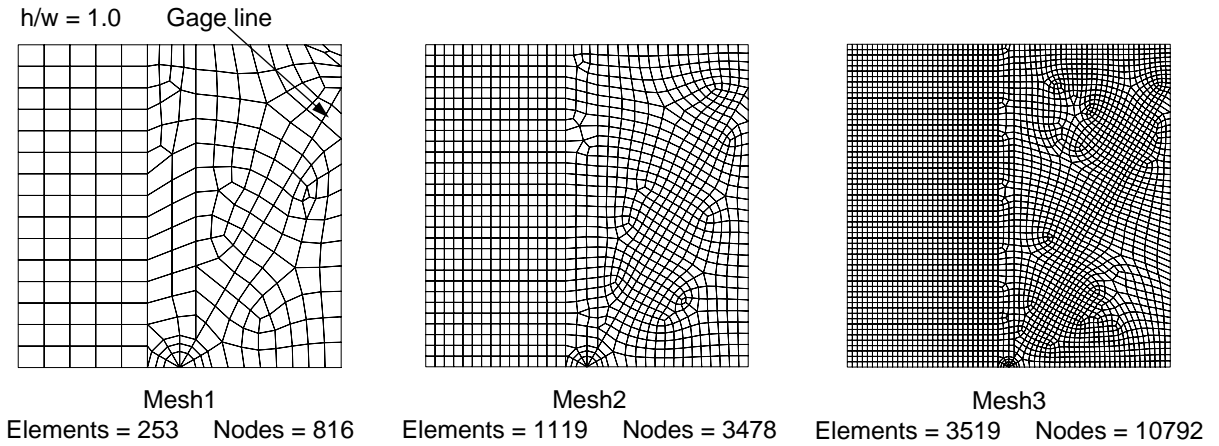


**Figure 6.** Different finite element meshes used for convergence study of  $r_{max}$  of  $a/w = 0.5$  and  $h/w = 1.0$  edge cracked configuration.

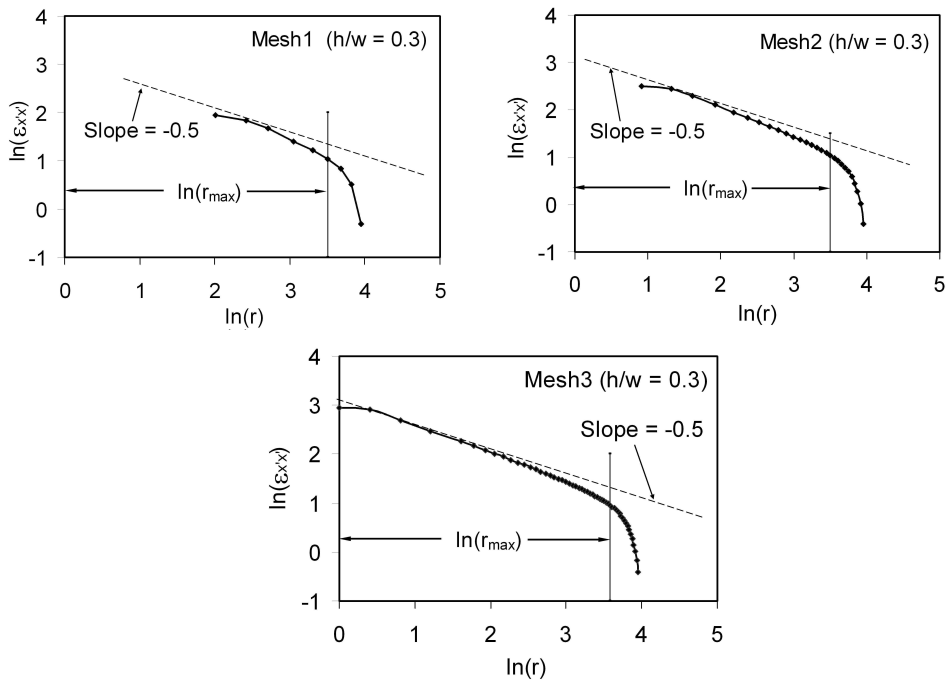


**Figure 7.** Linear and nonlinear variation of  $\ln(\varepsilon_{x'x'})$  with  $\ln(r)$  along the gage line for the sequence of meshes ( $a/w = 0.5$ ,  $h/w = 0.3$ ,  $\nu = 1/3$ ) shown in Figure 4.

Table 1 presents the values of  $r_{max}$  obtained from the graphs of Figures 7 and 8. The convergence of  $\log(\varepsilon_{x'x'})$  along the gage line for increasing mesh density of all the configurations is shown in Figure 9 along with the line of slope  $-0.5$ . No significant improvement of  $\log \varepsilon_{x'x'}$  values along the gage line can be noticed in Figure 9 for any configuration. As a result no noticeable differences in values of  $r_{max}$  can be

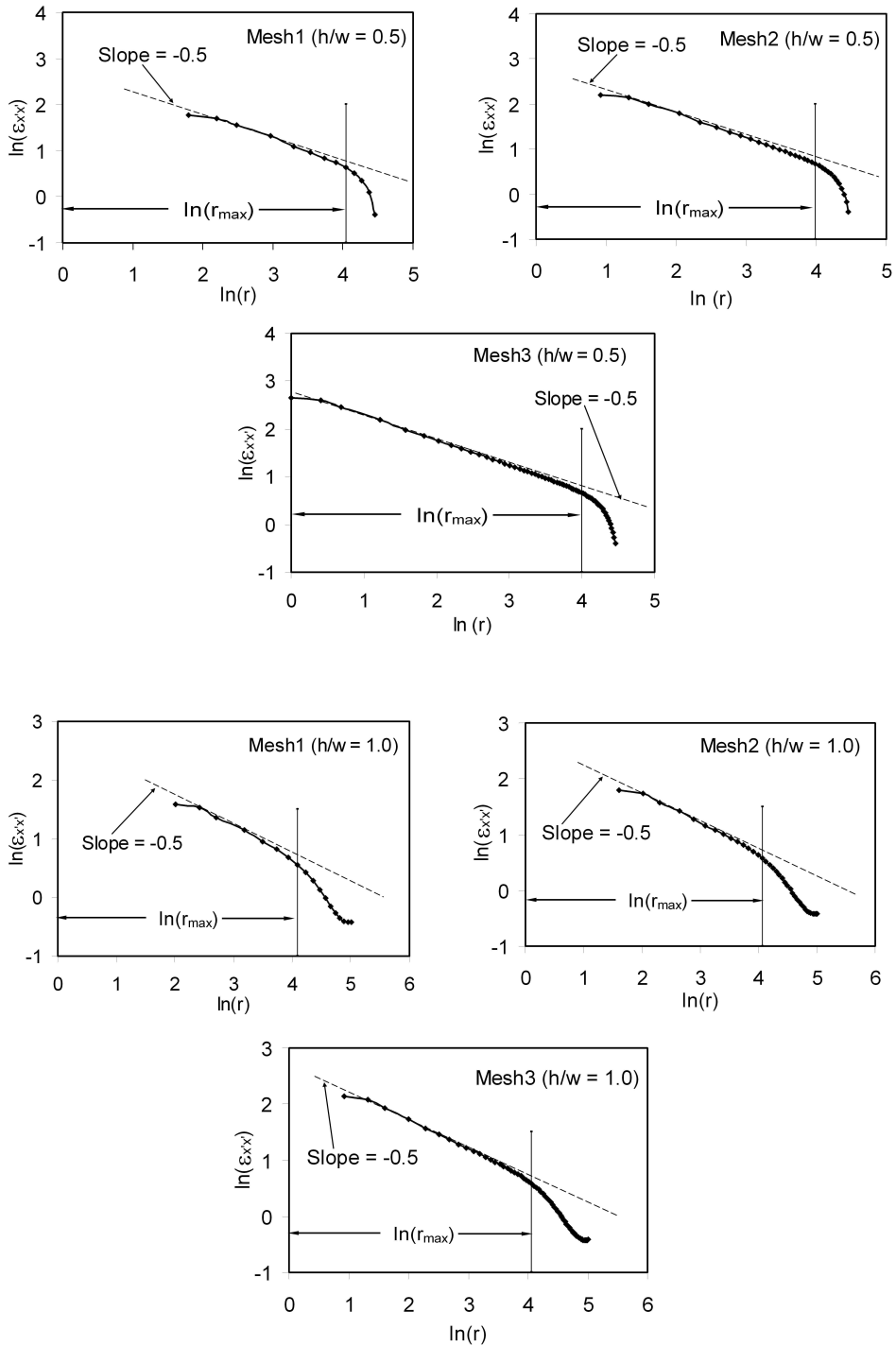


**Figure 8.** Variation of  $\ln(\epsilon_{x'x'})$  with  $\ln(r)$  along the gage line for the sequence of meshes ( $a/w = 0.5, h/w = 0.5, \nu = 1/3$ ) of Figure 5 (top three graphs) and the sequence of meshes ( $a/w = 0.5, h/w = 1.0, \nu = 1/3$ ) of Figure 6 (bottom graphs).

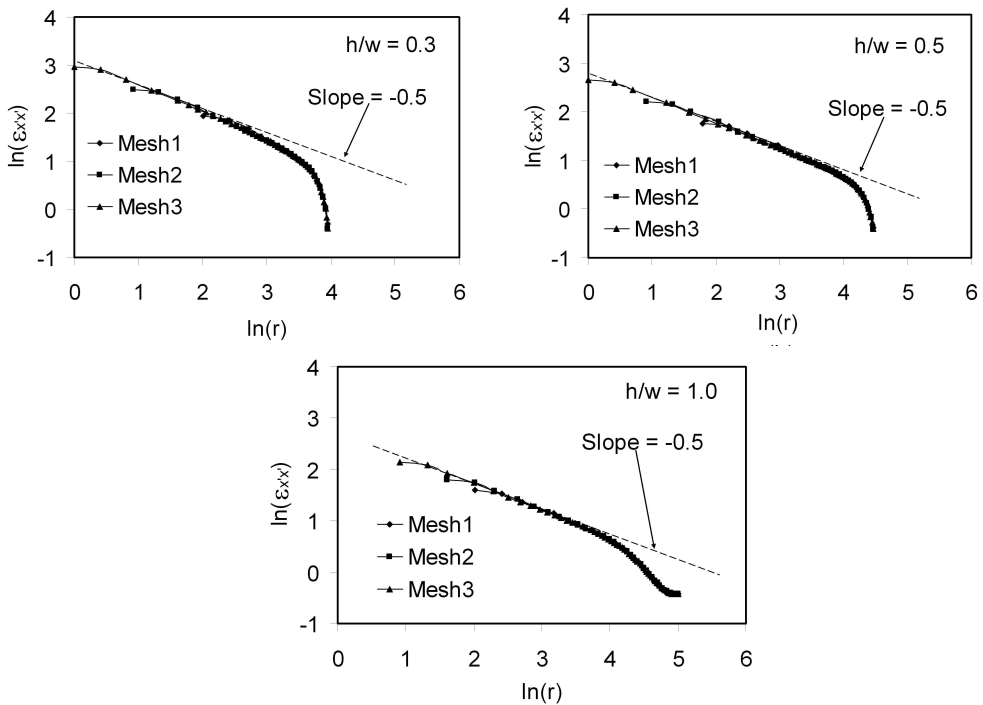


**Figure 9.** Convergence of  $r_{max}$  with the mesh refinement of various edge cracked configurations, with  $a/w = 0.5$ .

observed as the meshes are refined. The results presented in Figure 9 and Table 1 lead to the conclusion that a single finite element mesh with a reasonable density appropriate to the given configuration is sufficient to provide a fairly accurate value of  $r_{max}$ .

Next, in order to demonstrate the effect of Poisson’s ratio on values of  $r_{max}$ , two edge cracked plates having  $a/w = 0.5$ ,  $h/w = 0.3$  and having different Poisson’s ratios ( $\nu = 0.25$  and  $0.3$ ) is considered. Figure 10 shows corresponding finite element mesh of the domain having  $\nu = 0.25$  for determination of  $r_{max}$ . It can be noticed from (8) and (10) that, not only the values of  $\theta$  and  $\alpha$  would change because of change in the Poisson’s ratio but also the magnitude of  $\epsilon_{x'x'}$  at every point on the gage line. Corresponding to  $\nu = 0.25$  the values of  $\theta$  and  $\alpha$  are  $73.74^\circ$  and  $63.43^\circ$  respectively — see (9) and (10). Figure 11 shows the variation of  $\epsilon_{x'x'}$  (and hence  $r_{max}$ ) with Poisson’s ratio on the logarithmic axes. The results obtained

	$h/w = 0.3$		$h/w = 0.5$		$h/w = 1.0$	
	$r_{max}$ (mm)	$r_{max}/w$	$r_{max}$ (mm)	$r_{max}/w$	$r_{max}$ (mm)	$r_{max}/w$
Mesh1	33.5	0.22	56.8	0.38	60.0	0.40
Mesh2	33.2	0.22	54.0	0.36	58.0	0.39
Mesh3	36.0	0.24	55.6	0.37	58.2	0.39

**Table 1.** Convergence of  $r_{max}$  with the mesh refinement of different edge cracked specimens ( $a/w = 0.5$ ).

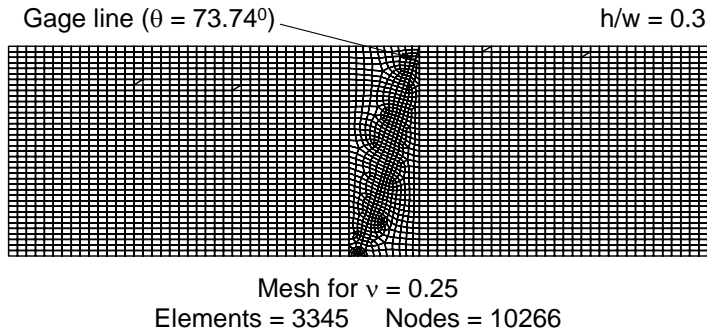


**Figure 10.** A fine mesh finite idealization of the edge cracked configuration with  $a/w = 0.5$ ,  $h/w = 0.3$  (Figure 3) and Poisson’s ratio = 0.25.

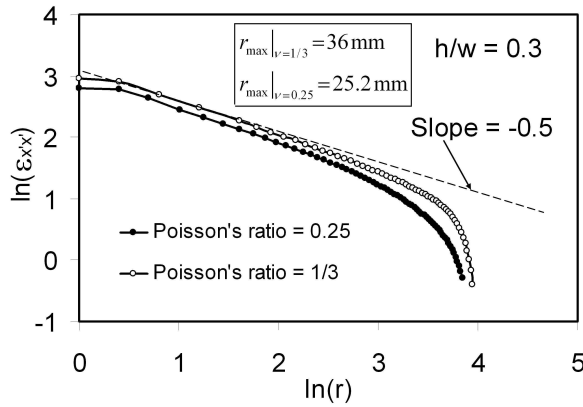


**Figure 11.** Variation of  $r_{\max}$  with the Poisson’s ratio.

using the meshes in Figure 4(c) and Figure 10 are employed to plot the graphs of Figure 11. These results appear to show that higher is the value of  $\nu$ , the larger is  $r_{\max}$ , indicating that the finite element analysis of a single mesh of the experimental configuration with exact material properties can aid in obtaining reasonably accurate values of  $r_{\max}$  graphically.

**Example 2: Dependence of the extent of the three parameter zone on the crack length.** The goal of this example is to demonstrate effect of the crack length on the value of  $r_{\max}$ . For this purpose the problem of edge cracked plate having  $h/w = 1.0$  and different values of  $a/w = 0.5, 0.6, 0.7, 0.8$  subjected to uniform tensile stress (Figure 3(a)) is chosen. A Poisson’s ratio of  $\nu = 1/3$  and an applied stress value of 1.0 MPa are assumed for all the configurations. Only one finite element mesh (fine mesh) of each of the above configurations is employed in the analysis. Figure 12 shows fine meshes of the edge cracked plates with  $a/w = 0.6, 0.7, 0.8$ . The third mesh in Figure 6 is employed for  $a/w = 0.5$ .

Figure 13 shows the variation of  $\log \epsilon_{x'x'}$  with  $\log r$  on the gage line of each configuration. It also shows the extent of validity of the three-parameter zone, that is, the value  $r_{\max}$  of the edge cracked plate as the crack length is increased. These values of  $r_{\max}$  are shown in Table 2. The results in this figure and table indicate that the extent of three-parameter zone decreases as the crack length increases. In other words,

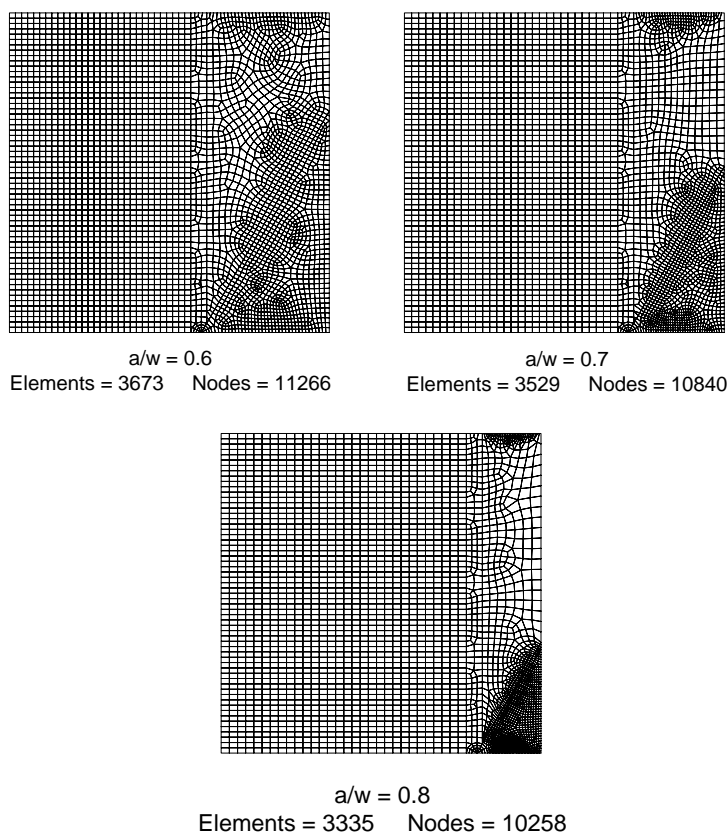


**Figure 12.** Finite element meshes of edge cracked plates with increasing crack length ( $h/w = 1.0$ ).

as the cracked domain becomes more finite, the  $r_{\max}$  value decreases. The same observation can be made from the results of [Table 1](#), and a similar conclusion was reached by [Chona et al. \[1983\]](#) using photoelastic studies, applied to the singular solutions in an effort to identify the singularity-dominated zone.

$a/w$	$r_{\max}$ (mm)	$r_{\max}/w$
0.5	58.2	0.39
0.6	35.7	0.24
0.7	27.7	0.18
0.8	15.1	0.10

**Table 2.** Variation of  $r_{\max}$  with  $a/w$  ( $h/w = 1.0$ ).

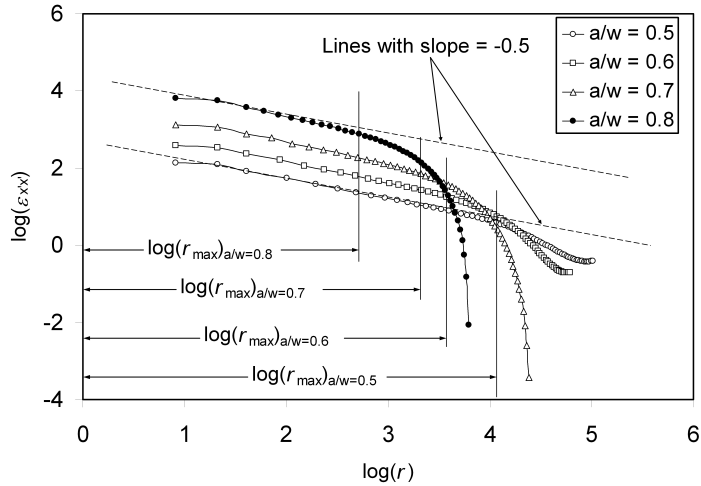


**Figure 13.** Dependence of the extent of the three-parameter zone on length of the crack.

### Conclusions

The present work outlines the theoretical basis for determination of  $r_{\max}$  in accordance with the single strain gage method of [Dally and Sanford 1987] which in turn can be used to justify the selected radial location of the gages. The present work attempts to propose a method of finding the reasonably accurate  $r_{\max}$  of a given experimental specimen using the finite element analysis. The numerical examples clearly demonstrate that reasonably accurate values of  $r_{\max}$  can be determined using the proposed approach. The dependence of  $r_{\max}$  on the geometry of the specimen and Poisson's ratio is demonstrated.

### Acknowledgements

Murthy acknowledges the support from Naval Research Board (NRB), Ministry of Defence, India. The authors sincerely thank the reviewers of this article, who provided valuable comments.

### References

- [Baik et al. 1995] M. C. Baik, S. H. Choi, J. S. Hawong, and J. D. Kwon, "Determination of stress-intensity factors by the method of caustics in anisotropic materials", *Exp. Mech.* **35**:2 (1995), 137–143.
- [Barsoum 1976] R. S. Barsoum, "On the use of isoparametric finite elements in linear fracture mechanics", *Int. J. Numer. Methods Eng.* **10**:1 (1976), 25–37.
- [Berger and Dally 1988] J. R. Berger and J. W. Dally, "An overdeterministic approach for measuring  $K_I$  using strain gages", *Exp. Mech.* **28**:2 (1988), 142–145.
- [Bonesteel et al. 1978] R. M. Bonesteel, D. E. Piper, and A. T. Davinroy, "Compliance and  $K_I$  calibration of double cantilever beam (DCB) specimens", *Eng. Fract. Mech.* **10**:2 (1978), 425–428.
- [Chan and Chow 1979] W. Y. Chan and C. L. Chow, "Photoelastic stress intensity determination of circular-sector crack in rectangular plate", in *Papers: SESA Spring Meeting* (San Francisco, 1979), Society for Experimental Stress Analysis, Westport, CT, 1979.
- [Chona et al. 1983] R. Chona, G. R. Irwin, and R. J. Sanford, "The influence of specimen size and shape on the singularity-dominated zone", pp. 1–23 in *Fracture mechanics: fourteenth symposium, I: Theory and analysis* (Los Angeles, 1981), edited by J. C. Lewis and G. Sines, ASTM Special Technical Publication **791**, ASTM, Philadelphia, 1983.

- [Dally and Berger 1993] J. W. Dally and J. R. Berger, "The role of the electrical resistance strain gauge in fracture research", pp. 1–39 in *Experimental techniques in fracture mechanics*, edited by J. S. Epstein, Wiley VCH, New York, 1993.
- [Dally and Sanford 1987] J. W. Dally and R. J. Sanford, "Strain-gage methods for measuring the opening-mode stress-intensity factor,  $K_I$ ", *Exp. Mech.* **27**:4 (1987), 381–388.
- [Gdoutos and Theocaris 1978] E. E. Gdoutos and P. S. Theocaris, "A photoelastic determination of mixed-mode stress-intensity factors", *Exp. Mech.* **18**:3 (1978), 87–96.
- [Hyde and Warrior 1990] T. H. Hyde and N. A. Warrior, "An improved method for determination of photoelastic stress intensity factors using the Westergaard stress function", *Int. J. Mech. Sci.* **32**:3 (1990), 265–273.
- [Kazemi et al. 1989] A. D. A. Kazemi, N. S. Murthy, and N. G. Raju, "Stress intensity factor determination of radially cracked circular rings subjected to tension using photoelastic technique", *Eng. Fract. Mech.* **32**:3 (1989), 403–408.
- [Konsta-Gdoutos 1996] M. Konsta-Gdoutos, "Limitations in mixed-mode stress intensity factor evaluation by the method of caustics", *Eng. Fract. Mech.* **55**:3 (1996), 371–382.
- [Kuang and Chen 1995] J. H. Kuang and L. S. Chen, "A single strain gage method for  $K_I$  measurement", *Eng. Fract. Mech.* **51**:5 (1995), 871–878.
- [Lee and Hong 1993] O. S. Lee and S. K. Hong, "Determination of stress intensity factors and  $J$ -integrals using the method of caustics", *Eng. Fract. Mech.* **44**:6 (1993), 981–989.
- [Marloff et al. 1971] R. H. Marloff, M. M. Leven, T. N. Ringler, and R. L. Johnson, "Photoelastic determination of stress-intensity factors", *Exp. Mech.* **11**:12 (1971), 529–539.
- [Newman 1981] J. C. Newman, Jr., "Stress-intensity factors and crack-opening displacements for round compact specimens", *Int. J. Fract.* **17**:6 (1981), 567–578.
- [Nurse et al. 1994] A. D. Nurse, E. W. O'Brien, and E. A. Patterson, "Stress intensity factors for cracks at fastener holes", *Fatigue Fract. Eng. Mater. Struct.* **17**:7 (1994), 791–799.
- [Rosakis and Ravi-Chandar 1986] A. J. Rosakis and K. Ravi-Chandar, "On crack-tip stress state: an experimental evaluation of three-dimensional effects", *Int. J. Solids Struct.* **22**:2 (1986), 121–134.
- [Sanford 1979] R. J. Sanford, "A critical re-examination of the Westergaard method for solving opening-mode crack problems", *Mech. Res. Commun.* **6**:5 (1979), 289–294.
- [Sanford 2003] R. J. Sanford, *Principles of fracture mechanics*, Prentice Hall, Upper Saddle River, NJ, 2003.
- [Swamy et al. 2008] S. Swamy, M. V. Srikanth, K. S. R. K. Murthy, and P. S. Robi, "Determination of mode I stress intensity factors of complex configurations using strain gages", *J. Mech. Mater. Struct.* **3**:7 (2008), 1239–1255.
- [Theocaris 1970] P. S. Theocaris, "Local yielding around a crack tip in Plexiglas", *J. Appl. Mech. (ASME)* **37** (1970), 409–415.
- [Wei and Zhao 1997] J. Wei and J. H. Zhao, "A two-strain-gage technique for determining mode I stress-intensity factor", *Theor. Appl. Fract. Mech.* **28**:2 (1997), 135–140.

Received 18 Aug 2008. Revised 7 Sep 2008. Accepted 22 Sep 2008.

B. KAUSHIK: [kauaug18@gmail.com](mailto:kauaug18@gmail.com)

Tata Motors Limited, Pune, India

K. S. R. K. MURTHY: [ksrkm@iitg.ernet.in](mailto:ksrkm@iitg.ernet.in)

Department of Mechanical Engineering, Indian Institute of Technology Guwahati, Guwahati - 781 039, Assam, India

P. S. ROBI: [psr@iitg.ernet.in](mailto:psr@iitg.ernet.in)

Department of Aerospace Engineering, Indian Institute of Space Science and Technology, Thiruvananthapuram - 695 022, India